Electronic Supplementary Material (ESI) for Journal of Materials Chemistry B.

Low fouling and ultrasensitive electrochemical immunosensor with dual assay methods based on Fe_3O_4 magnetic nanoparticles

Wenshi Li [a], Gao-Chao Fan [a], Xiaojian Fan [b], Ruiqiao Zhang [a,c], Lei Wang [a], Wei Wang [a], Xiliang Luo [a,*]

[a] Key Laboratory of Sensor Analysis of Tumor Marker, Ministry of Education, College of Chemistry and Molecular Engineering, Qingdao University of Science and Technology, Qingdao 266042, China

[b] Department of Breast Surgery, The Eighth People's Hospital of Qingdao, Qingdao 266100, China

[c] Qingdao Academy of Agricultural Sciences, Qingdao 266100, China

* Corresponding Author. E-mail address: xiliangluo@qust.edu.cn

Section 1: DLS dates

Section 2: Electrochemical dates

Section 3: SEM images of the electrochemical conversion

Section 4: Optimization of the electrochemical biosensor

Section 5: Contact angle measurement of electrode surfaces

Section 6: Table S1

Section 7: Table S2

Section 8: References

Section 1: DLS dates

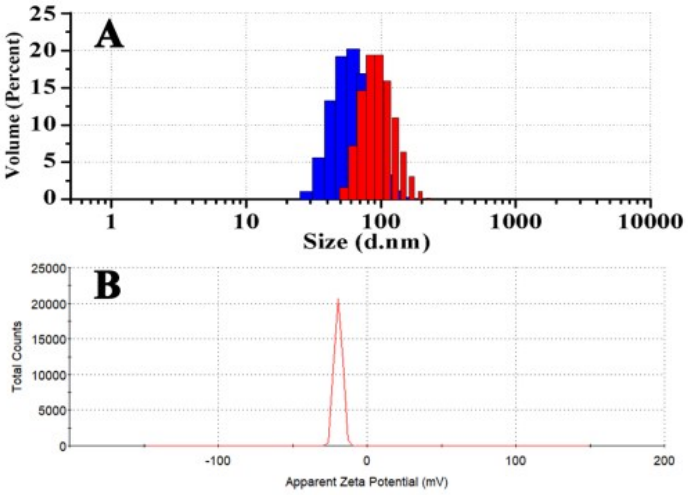

Fig. S1. (A) Size distribution histogram of Fe_3O_4 before (blue column) and after (red column) conjugation with antigen measured with DLS. (B) Zeta potential of Fe_3O_4.

Section 2: Electrochemical dates

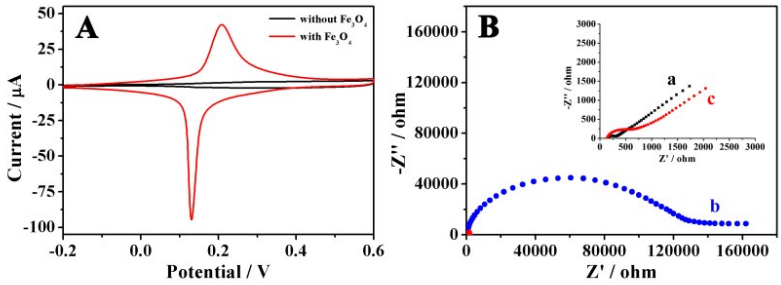

Fig. S2. (A) CV curves of magnetic gold electrodes (MAu) with and without Fe_3O_4@Ag treated by electrochemical conversion process. (B) EIS plots of (a) bare magnetic gold electrode, (b) Fe_3O_4@Ag/MAu and (c) Fe_3O_4@Ag/MAu after electrochemical conversion. Inset shows the magnified part of the EIS plot.

Section 3: SEM images of the electrochemical conversion

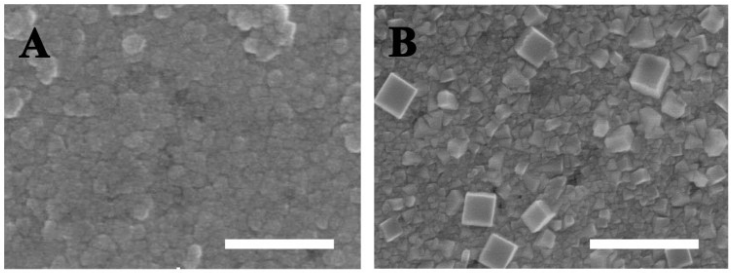

Fig. S3. SEM images of the Fe_3O_4@Ag conjugated gold electrode before (A) and after (B) the electrochemical conversion. Scale bares represent 500 nm.

Section 4: Optimization of the electrochemical biosensor

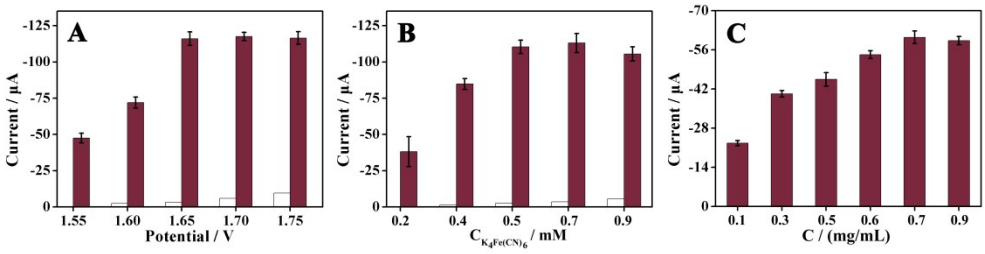

Fig. S4. Effects of (A) potentials and (B) concentrations of $K_4Fe(CN)_6$ on the electrochemical conversion process (open columns are controls without magnetic nanoparticles), and (C) Effect of Fe_3O_4@Ag concentration on the competitive immunoassay.

High potential is an important factor for the electrochemical conversion of magnetic nanoparticles. To maximize the sensitivity of the electrochemical immunosensor, the high potential was optimized using SWV, as shown in Fig. S4 A. It can be clearly observed that the reduction peak current increases with the increasing potential and arrives at a maximum at 1.65 V (filled column). In the control experiment, the reduction peak currents were measured in the absence of magnetic nanoparticles (open column), the reduction peak current increases

gradually with the increase of the high potential. Thus 1.65V was used as the high potential in the electrochemical conversion process. The concentrations of $K_4Fe(CN)_6$ for this electrochemical conversion process was optimized in the same way and fixed at 0.5 mM (Fig. S4 B).

Concentration of Fe_3O_4@Ag is another important factor influencing the signal response in this assay. The more Fe_3O_4@Ag was conjugated on electrode surface, the more electroactive PB analogues can be generated. Various concentrations of Fe_3O_4@Ag were used to conjugate with antibodies based on the specific antigen-antibody recognition reaction. As shown in Fig. S4 C, the maximum peak currents for the "signal-off" method were obtained at 0.7 mg/mL, which was used as the optimal concentration of Fe_3O_4@Ag for the following experiments.

Section 5: Contact angle measurement of electrode surfaces

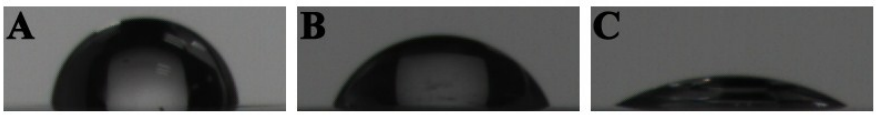

Fig. S5. Contact angle measurement of (A) bare Au, (B) Ab/Au, (C) Ab/MCH/PEG/Au surfaces.

Section 6:

Table S1. Comparison of various sensing techniques for CA 15-3 detection

Technique	Linear range	LOD	*Ref.*
Electrochemiluminescence	0.0005 - 500 U/mL	20 μU/mL	*1*
Electrochemistry	0.01 - 50 U/mL	0.005 U/mL	*2*
Electrochemistry	20 μU/mL-40 U/mL	5 μU/mL	*3*
Electrochemistry	10 - 1000 μU/mL	6 μU/mL	*4*
Localized Surface Plasmon Resonance	0.38 - 8.9 U/mL	0.11 U/mL	*5*
Plasmon-enhanced Raman	0.1 - 500 U/mL	0.99 U/mL	*6*
Electrochemiluminescence	0.0001 - 100 U/mL	10 μU/mL	*7*
Electrochemistry	1.0 μU/mL-0.1U/mL	0.41 μU/mL	*this work*

Section 7:

Table S2. Contact angle measurement of bare Au, Ab/Au and Ab/MCH/PEG/Au surfaces.

	Contact angle (°)		
	Bare Au	Ab/Au	Ab/MCH/PEG/Au
1	75.88	60.98	28.33
2	75.70	58.76	28.73
3	75.53	61.27	27.67
Average	75.71	60.33	28.25

Section 8: References

1. H. Ke, X. Zhang, C. S. Huang and N. Q. Jia, *Biosens. Bioelectron.*, 2018, **103**, 62-68.
2. D. P. Tang, L. Hou, R. Niessner, M. D. Xu, Z. Q. Gao and D. Knopp, *Biosens. Bioelectron.*, 2013, **46**, 37-43.
3. S. G. Ge, X. L. Jiao and D. R. Chen, *Analyst.*, 2012, **137**, 4440-4447.
4. R. A. G. de Oliveira, E. M. Materon, M. E. Melendez, A. L. Carvalho and R. C. Faria, *ACS Appl. Mater. Interfaces*, 2017, **9**, 27433-27440.
5. O. Yavas, S. S. Acimovic, J. Garcia-Guirado, J. Berthelot, P. Dobosz, V. Sanz and R. Quidant, *ACS Sens.*, 2018, **3**, 1376-1384.
6. M. Li, J. W. Kang, S. Sukumar, R. R. Dasari and I. Barman, *Chem. Sci.*, 2015, **6**, 3906-3914.
7. B. Babamiri, R. Hallaj and A. Salimi, *Biosens. Bioelectron.*, 2018, **99**, 353-360.